Materials Chemistry and Physics 155 (2015) 67–75

Contents lists available at ScienceDirect

Materials Chemistry and Physics

journal homepage: www.elsevier.com/locate/matchemphys

Structural transformations of heat-treated bacterial iron oxide

Hideki Hashimoto [a, b, *], Tatsuo Fujii [a], Shinji Kohara [c], Koji Nakanishi [d], Chihiro Yogi [e], Herwig Peterlik [f], Makoto Nakanishi [a], Jun Takada [a, b]

[a] *Graduate School of Natural Science and Technology, Okayama University, Okayama 700-8530, Japan*
[b] *JST, CREST, Okayama 700-8530, Japan*
[c] *Japan Synchrotron Radiation Research Institute, Sayo, Hyogo 679-5198, Japan*
[d] *Office of Society-Academia Collaboration for Innovation, Kyoto University, Uji 611-0011, Japan*
[e] *SR Center, Ritsumeikan University, Kusatsu, Shiga 525-8577, Japan*
[f] *Faculty of Physics, University of Vienna, A-1090 Vienna, Austria*

HIGHLIGHTS

- Structural transformation of a bacterial iron oxide microtubule was investigated.
- Si—O—Fe was cleaved with increasing temperature to form α-Fe_2O_3/silicate composite.
- Crystallization to 2Fh started at 500 °C to give α-Fe_2O_3 >700 °C.
- FeO_6 octahedra were highly distorted <500 °C.
- Formation of face-sharing FeO_6 was promoted >500 °C, releasing the local strain of FeO_6.

GRAPHICAL ABSTRACT

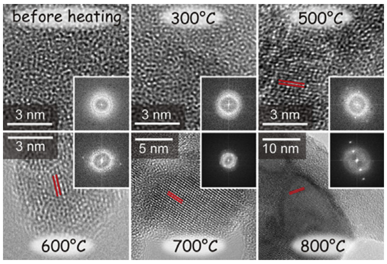

ARTICLE INFO

Article history:
Received 24 May 2014
Received in revised form
24 December 2014
Accepted 31 January 2015
Available online 7 February 2015

Keywords:
Amorphous materials
Composite materials
Nanostructures
Oxides

ABSTRACT

A bacterial siliceous iron oxide microtubule (diameter: *ca.* 1 μm, $15Fe_2O_3 \cdot 8SiO_2 \cdot P_2O_5 \cdot 30H_2O$) produced by *Leptothrix ochracea* was heat treated in air and its structural transformation was investigated in detail by microscopy, diffractometry, and spectroscopy. Although the heat-treated bacterial iron oxide retained its original microtubular structure, its nanoscopic, middle-range, and local structures changed drastically. Upon heat treatment, nanosized pores were formed and their size changed depending on temperature. The Fe—O—Si linkages were gradually cleaved with increasing temperature, causing the progressive separation of Fe and Si ions into iron oxide and amorphous silicate phases, respectively. Concomitantly, global connectivity and local structure of FeO_6 octahedra in the iron oxide nanoparticles systematically changed depending on temperature. These comprehensive investigations clearly revealed various structural changes of the bacterial iron oxide which is an important guideline for the future exploration of novel bio-inspired materials.

1. Introduction

Inorganic nanomaterials and nanostructured materials are at the leading-edge of material research and development. For example, nanosizing and nanostructuring of electrode materials for Li-ion batteries achieve high capacity, excellent cyclability, and rate

---

* Corresponding author. Graduate School of Natural Science and Technology, Okayama University, Okayama 700-8530, Japan.
E-mail address: hideki-h@cc.okayama-u.ac.jp (H. Hashimoto).

http://dx.doi.org/10.1016/j.matchemphys.2015.01.067
0254-0584/© 2015 Elsevier B.V. All rights reserved.

capability compared with bulk materials [1–4]. In catalytic chemistry, nanosized metal particles dispersed over oxide supports have found use in many industries [5]. The generation of mesoporous structures has also facilitated the development of new catalytic reactions [6–9]. However, these approaches generally require complicated, costly, and energy-consuming fabrication processes that hinder their practical application. As a departure from these conventional materials' explorations, this report focuses on oxide materials (*e.g.*, iron oxides and manganese oxides) produced by microorganisms under mild and low-energy consumption conditions [10,11].

Nanometric amorphous iron oxides formed by iron-oxidizing bacteria [10,11], *i.e.*, biogenous iron oxides (BIOXs), exhibit unique properties. Silicon-containing BIOX formed by *Leptothrix ochracea* [12] (*L*-BIOX; chemical composition: $15Fe_2O_3 \cdot 8SiO_2 \cdot P_2O_5 \cdot 30H_2O$ [13]) displays a nano/microstructure that primarily consists of ~3 nm nanoparticles [14]. These primary particles aggregate into secondary fibrillar and globular structures measuring several tens of nanometers that are intricately interconnected into a *ca.* 1 μm diameter microtubule [15]. In addition, these structures contain a small amount of bacterial saccharic polymers in their core, resulting in an inorganic/organic nanohybrid material [15]. Produced by simple exposure of natural iron-containing groundwater to the outside environment, this ubiquitous and cost-effective material surprisingly presents a wide variety of functions and is convertible into various materials. *L*-BIOX exhibits nanometric, amorphous, and compositional features, making it a good candidate as a Li-ion battery anode [16]. It also expected to serve as an excellent catalyst scaffold because of its large surface area (280 m^2/g) and numerous surface OH groups [14,17]. *L*-BIOX can easily be converted into beautiful red pigments [18], magnetic materials [19,20], and amorphous acid silica [21] through very simple post-treatments.

L-BIOX has been found to undergo the phase separation into crystalline iron oxide and amorphous silicate phases by heat treatment [18–20]. In addition to the original functions of *L*-BIOX, products formed at various heat-treatment temperatures are expected to display new functions because their composite architecture present nano/microstructural features. The development of BIOX-based materials and new bio-inspired materials hinges on a deep understanding of the structural changes of BIOXs during heat treatment. This study aims at elucidating the heat-induced structural transformation of *L*-BIOX at microscopic, middle-range, and local levels in a comprehensive manner using different analytical methods.

2. Experimental

2.1. Sampling and heat treatments

L-BIOX was collected from an enrichment culture tank in Joyo city near Kyoto, Japan, and centrifuge-washed several times using distilled water to remove groundwater-derived impurities, as described in our previous reports [13–21]. The washed *L*-BIOX was dried *in vacuo* at room temperature, heat-treated at temperatures ranging between 100 and 800 °C in air for 2 h at a heating rate of 10 °C min^{-1}, and allowed to cool in the furnace. The unheated powder and resulting heat-treated powders were subjected to the following analytical methods.

2.2. Thermogravimetric/differential thermal analysis (TG/DTA) measurements

TG/DTA measurements of the unheated sample were performed in air by heating to 1000 °C at a rate of 10 °C min^{-1} using a TG8120 instrument (Rigaku, Japan).

2.3. X-ray diffraction (XRD) measurements

XRD patterns of unheated and heated samples were obtained on a RINT-2000 diffractometer (Rigaku, Japan) using a monochromated CuKα radiation.

2.4. Electron microscopy measurements

Scanning electron microscopy (SEM) measurements were performed on a Hitachi S-4300 microscope. The samples were coated with evaporated platinum prior to measurements. Transmission electron microscopy (TEM) and scanning transmission electron microscopy (STEM) measurements were conducted on a JEM-2100F microscope (JEOL, Japan) equipped with a spherical aberration corrector (C_s-corrector, CEOS, Germany) for condenser lens at an acceleration voltage of 200 kV. The sample powders were dispersed on a carbon-coated copper grid. The C_s-corrector was not used during high resolution TEM imaging. When secondary electron (SE) images and high-angle annular dark-field (HAADF) images were acquired by STEM, the C_s-corrector was used.

2.5. Measurements of nitrogen adsorption isotherms

Nitrogen adsorption isotherms were measured at 77 K using a BELSORP-mini-II system (BEL Japan) to determine the surface area and pore size distribution. Prior to measurements, every sample was degassed under vacuum for 4 h at 100 °C. Data were analyzed by the Brunauer–Emmet–Teller (BET) method to estimate the surface area [22] and the Dollimore–Heal method to obtain pore size distribution [23,24].

2.6. In-situ small angle X-ray scattering (SAXS) measurements

In-situ SAXS measurement of the unheated sample was performed using a pinhole camera equipped with a rotating anode generator. Cross-coupled Göbel mirrors (Nanostar, Bruker, Germany) were used to collimate and monochromate the CuKα radiation. The unheated sample was heat-treated at temperatures ranging from 100 to 800 °C in 100 °C increments for 1 h at a heating rate of 10 °C min^{-1} in air in a furnace positioned inside the diffractometer chamber. SAXS patterns were acquired at specimen–detector distance of 1.07 m using a two-dimensional position sensitive detector (Vantec 2000, Bruker, Germany), radially averaged, and corrected for background scattering. Thus, scattering intensities were obtained in dependence on the scattering vector q with $q = 4\pi \sin\theta/\lambda$, where 2θ is the scattering angle and λ is the X-ray wavelength ($\lambda = 0.1542$ nm).

2.7. Fourier transform infrared (FTIR) spectroscopy measurements

FTIR spectra of the samples were recorded in transmission mode at room temperature on a thin pelletized sample using a FT/IR-4100 spectrometer (JASCO, Japan).

2.8. Si and P K-edge X-ray absorption fine structure (XAFS) measurements

Si and P K-edge X-ray absorption near edge structure (XANES) spectra of the samples were recorded using a double-crystal monochromator beamline (BL-10, SR center, Ritsumeikan University, Japan) [25]. Each sample was installed in the instrument chamber using a carbon tape, and the spectrum was obtained with the total electron yield mode under high vacuum condition.